Nuclear Engineering and Design 265 (2013) 232–243

Contents lists available at ScienceDirect

Nuclear Engineering and Design

journal homepage: www.elsevier.com/locate/nucengdes

Stability of self-pressurized, natural circulation, low thermo-dynamic quality, nuclear reactors: The stability performance of the CAREM-25 reactor

C.P. Marcel[a,b,c,*], F.M. Acuña[a,b], P.G. Zanocco[a,b], D.F. Delmastro[a,b]

[a] Instituto Balseiro, 8400 S. C. de Bariloche, Argentina
[b] Centro Atómico Bariloche, CNEA, Bustillo 9500, 8400 S. C. de Bariloche, Argentina
[c] Consejo Nacional de Investigaciones Científicas y Técnicas (CONICET), Argentina

HIGHLIGHTS

- By increasing the condensation power the reactor becomes more stable.
- The reactor stability is degraded when the two-phase limit is within the first half of the chimney.
- It is observed by decreasing the pressure the system becomes less stable.
- The model predicts CAREM-25 can be started up safely if a minimum condensation power is guaranteed.

ARTICLE INFO

Article history:
Received 4 February 2013
Received in revised form 23 July 2013
Accepted 15 August 2013

ABSTRACT

The stability performance of self-pressurized, natural circulation, low-thermodynamic quality, nuclear reactors such as CAREM-25 is very different from existing conventional nuclear reactors. In this work, the linear stability of such a reactor is investigated in depth for both, nominal and low pressure-low power (start-up) conditions. As a result it is found that the flashing effect is crucial to correctly investigate the stability performance of the CAREM-25 reactor. In addition, it is verified that the dominant destabilizing mechanism are density waves travelling through the chimney section corresponding to Type-I instabilities. From the results it is observed that at rated conditions the unstable region is only limited to cases in which the two-phase boundary is located within a region which extends approximately from the core outlet until the middle of the chimney. It is also found that the condensation taking place in the steam dome has a great impact in defining the stability of the reactor and thus can be used to tune the CAREM-25 operational point. It is observed that the reactor shows a better stability performance when increasing the system pressure. From the steady state results it is found that the system could be pressurized without encountering instabilities if a certain minimum condensation power level is guaranteed.

1. Introduction

CAREM-25 is an Argentine project aimed to achieve the development, design and construction of an innovative, simple and small Nuclear Power Plant (NPP). This nuclear plant is modular and has some distinctive features which greatly simplify the design contributing to a higher safety level. Some of these features are: an integrated primary cooling system, natural circulation as the only mean of cooling the reactor core and self-pressurization of the primary system. The pressurization is achieved by balancing the vapor production in the hot leg (by means of boiling and flashing effect) and the condensation of vapor in contact with cold structures in the upper steam dome. The CAREM-25 concept was first presented in 1984 and was, chronologically, one of the first designs of the present new generation of reactors. CAREM-25 has been recognized as an International Near Term Deployment (INTD) reactor by the Generation IV International Forum (GIF) (Gomez, 2000).

Low quality natural circulation systems have been studied both in a numerical and in an experimental way in the past (Guanghui et al., 2002, 2001; Marcel et al., 2009). Despite these valuable works, none of those studied the case of self-pressurized systems as the one presented in this article. Moreover, different small integrated reactor designs exist, some of which are (partially) cooled by natural circulation low quality flows, which phenomenology was discussed in different works (Junli et al., 2006; Kusunoki et al., 2000; Iida et al., 1994; Lee, 2000). What makes CAREM-25 different,

* Corresponding author at: Instituto Balseiro, 8400 S. C de Bariloche, Argentina. Tel.: +54 2944 445101.
E-mail addresses: christian.marcel@cab.cnea.gov.ar, chris.p.marcel@gmail.com (C.P. Marcel).

0029-5493/$ – see front matter © 2013 Elsevier B.V. All rights reserved.
http://dx.doi.org/10.1016/j.nucengdes.2013.08.057

Nomenclature

Normal alphabet

a	amplification factor
A	reference cross section in the loop (m^2)
c_p	heat capacity (J/kg K)
g	gravity acceleration (m/s^2)
h	enthalpy of the liquid (J/kg)
K	localized friction coefficient
l	length (m)
$\dot{m}$	coolant flow in the circuit (kg/s)
N	non dimensional number
P	pressure at the steam dome (Pa)
Q	power (W)
r	feedback reactivity coefficient
t	time (s)

Greek letters

β	expansion coefficient (1/K)
λ	flashing-boiling boundary length (m)
ρ	density (kg/m^3)
χ	thermo-dynamic equilibrium quality

Subscripts

Cond	condensation in the steam dome
e	exit location
fg	liquid vapour phase change
i	inlet location
l	liquid
Nuc	core section
PCH	phase change
Sat	saturation
SG	steam generators
Sub	subcooled
Sys	system, entrance of the cooled section
v	vapour

though, is the fact it does not have any active system controlling the system pressure. Due to this, the interwoven phenomena involved in CAREM-25 promote a behaviour which is different than that from traditional LWRs (including the referenced designs). Such a difference has strong consequences in the reactor thermal-hydraulics (Marcel et al., 2013; Delmastro, 2008; IAEA, in press). From previous investigations (See references Marcel et al. (2013), Delmastro (2008) and IAEA (in press)) it has been shown in self-pressurized, natural circulation, low-thermodynamic quality, nuclear reactors (such as CAREM-25) the existing phenomena interact each other causing the resulting dynamics to be different from other reactors (e.g. PWRs, BWRs and also natural circulation BWRs). It is therefore obvious that the combination of complex effects makes CAREM-25 behaviour difficult to be extrapolated from existing knowledge. In particular, by using simple analytical relations Marcel et al. (2013) showed important characteristics which may have a great impact in the stability of the reactor. For this reason an exhaustive analysis regarding the thermal-hydraulic performance (including stability analysis) needs to be performed in order to thoroughly understand the behaviour of such a system. In a previous investigation, Zanocco et al. (2004a) presented the stability of CAREM-25 at nominal conditions. From such an investigation it has been found the CAREM-25 stability is strongly influenced by the steam-dome dynamics. Condensation in the steam zone, together with the reactor power, determines the dynamical state of the system. From a parametric study it is proved flashing plays a very important role in the reactor dynamics at nominal conditions. In addition, the steam-dome-pressure feedback is identified as a stabilizing effect. Despite this valuable work, no stability study has been performed at conditions different than nominal. In particular, it is expected that the stability performance of the CAREM-25 reactor could be diminished at start-up conditions, i.e. low pressure and low power conditions due, for instance, to the enhancement of the flashing effect. For this reason, stability investigations in a wide range of operational conditions need to be addressed in order to gain confidence regarding CAREM-25 thermal-hydraulic behaviour. Here, the thermal-hydraulic behaviour of a natural circulation, low quality, self-pressurized, integrated reactor is presented in both analytical and numerical ways.

2. The CAREM-25 reactor

2.1. Brief description

CAREM-25 is an indirect cycle reactor with some distinctive features that greatly simplify the design. The features which have a great impact on the stability performance of the reactor are:

- Integrated primary cooling system;
- Self-pressurization;
- Natural circulation due to low thermo-dynamic quality flow;

Despite these features, as an innovative reactor, the interactions between present phenomena need to be known in depth in order to guarantee a safe operation at any condition.

2.2. Primary circuit and its main characteristics

CAREM-25 design is based on a light water integrated reactor. The whole high energy primary system: core, steam generators, primary coolant and steam dome, is contained inside a single pressure vessel (RPV). Moreover the cooling primary flow is achieved by natural circulation induced by setting the steam generators above the core.

Fig. 1 shows a diagram of the coolant natural circulation in the primary system together with basic CAREM-25 technical data. Water enters the core from the lower plenum. After been heated, the coolant exits the core and flows up through the chimney to the upper steam dome. In the upper part, water leaves the chimney through lateral windows to the external region. It then flows down through modular steam generators, decreasing its enthalpy. Finally, the coolant exits the steam generators and flows down through the downcomer to the lower plenum, closing the circuit. The driving force created by the density differences along the circuit is balanced by the friction and form losses, producing the adequate flow rate in the core. Coolant also acts as neutron moderator.

Self-pressurization of the primary system in the steam dome is the result of the liquid–vapor equilibrium. In this way, typical heaters present in conventional PWRs are eliminated. The large vapor volume in the RPV also contributes to damping pressure perturbations.

The control rod-drive (CRD) mechanisms are hydraulically operated and they are located inside the RPV. Therefore, this design avoids the use of mechanical shafts passing through the RPV wall, which in turns eliminates the possibility of a control rod ejection and a large LOCA.

Due to self-pressurization, bulk temperature at core outlet is at saturation temperature at primary pressure. The continuous condensation promoted by the flow controlling the CRD and, to a lesser extent, by the RPV structures, ensures the thermo-dynamical coupling of the steam zone with the primary circuit. The negative reactivity feedback coefficients and the large water inventory of

Name	CAREM-25
Reactor type	PWR int.
Thermal power	100 MW(t)h
Electric power	27 MW(e)
Fuel type	LE UO_2
Cooling method	Nat. Circ.
Coolant volume	39 m3
Mass flow rate	410 Kg/s
Nominal pressure	12.25 MPa
Core outlet temp.	284 °C
Core inlet temp.	326 °C
Core height	1.4 m
Chimney height	4.6 m
N° of SG	12
Feedwater temp.	200 °C
Secondary pressure.	4.7 MPa

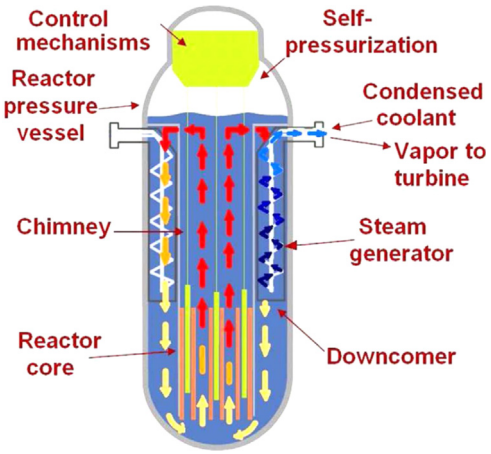

Fig. 1. The CAREM-25 reactor: schematic view of the flow circulation and basic data.

the primary circuit, combined with the self-pressurization features, support an excellent response under operational transients. Nevertheless, stability phenomena should be studied to guarantee this behaviour.

2.3. Relevant phenomena in CAREM-25 thermal-hydraulics

The physics involved in the CAREM-25 reactor includes different well known phenomena such us self-pressurization, flashing, natural circulation, condensation, density wave instabilities, neutronic coupling, etc. The combination of these, however, creates numerous feedbacks which influence the reactor dynamics creating novel situations which are potentially destabilizing and therefore need to be investigated in depth. In the following the aforementioned phenomena and their consequences are described which helps understanding the CAREM-25 behaviour.

2.3.1. Single-phase natural circulation

In CAREM-25 reactor the steam quality is very low and therefore the largest contribution driving term in the momentum balance is due to single-phase buoyancy forces. Due to this reason, in the following simplified analysis, only single-phase natural circulation is considered.

To estimate the mass flow rate, let us assume a single-phase closed loop with a uniformly heated section placed at the bottom of the upwards branch and a uniformly cooled section located at the top of the downwards branch, with all other sections isolated, see Fig. 2.

The length of the heated and cooled sections is $L1$ and $L2$ respectively while L is the vertical distance existing between them. A is the reference cross sectional area of the loop. To simplify the analysis a single friction coefficient K is used together with the Boussinesq approximation.

The mass flow rate in the loop can be obtained from the steady state momentum balance (see Marcel et al. (2013)). Thus

$$\dot{m} = \sqrt[3]{\frac{2A^2 Q_{Nuc} g \rho_l^2 \beta}{K c_p}\left[L + \frac{L1 + L2}{2}\right]} \tag{1}$$

where ρ_l is the fluid density at the exit of the heated part, β is the thermal expansion coefficient, g the acceleration of gravity, c_p is the fluid heat capacity and Q_{Nuc} is the nuclear power produced in the core. In addition, it can be shown the enthalpy increase in the core section is (see Marcel et al. (2013))

$$h_{Nuc,e} - h_{Nuc,i} = \Delta h = \frac{Q_{Nuc}}{\dot{m}} = \sqrt[3]{\frac{K c_p Q_{Nuc}^2}{2A^2 g \rho_l^2 \beta}\left[L + \frac{L1 + L2}{2}\right]^{-1}} \tag{2}$$

with $h_{Nuc,e}$ and $h_{Nuc,i}$ being the core exit and core inlet enthalpy.

2.3.2. The self-pressurization mechanism

In order to have a constant pressure in CAREM-25, some vapor needs to be created inside the RPV. This constrain fixes the core outlet temperature close to the saturation value. Assuming no carry under of bubbles exists in the downcomer, the vapor created in the hot leg is condensed before entering the cooling devices. The steady state energy balance for the entire circuit, yields

$$Q_{Nuc} = Q_{SG} + Q_{Cond} \tag{3}$$

where Q_{SG} is the power extracted by the cooling devices (i.e. the steam generators) and Q_{Cond} the power related with vapor condensation. Such a condensation takes place in the upper part of the reactor vessel and is a direct consequence of the heat losses and the interaction of the vapor with cold structures present in the steam dome such as those from the reactivity control drive (CRD) mechanism.

By using Eq. (2) and assuming the coolant at the core exit location is saturated, an expression for the core inlet enthalpy $h_{Nuc,i}$ can

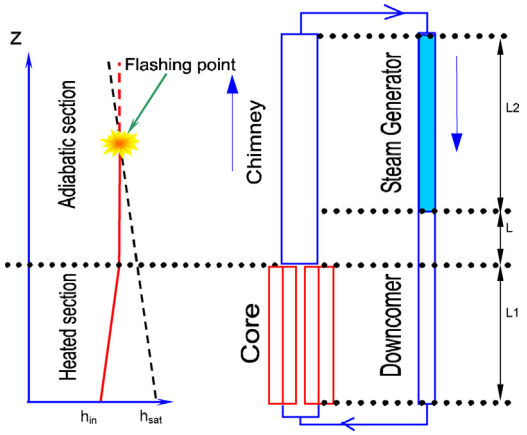

Fig. 2. Schematic of a closed circuit representing CAREM-25 and the occurrence of flashing.

be found.

$$h_{Nuc,i} = h_{l,sat} - (Q_{Nuc} - Q_{Cond}) \sqrt[3]{\frac{Kc_p}{2A^2 Q_{Nuc} g \rho_l^2 \beta} \left[L + \frac{L1 + L2}{2}\right]^{-1}} \quad (4)$$

where $h_{l,sat}$ refers to the liquid saturation enthalpy.

In the same way, the mean enthalpy in the reactor core, $\bar{h}_{Nuc}$, can be obtained.

$$\bar{h}_{Nuc} = h_{l,sat} - \left(\frac{Q_{Nuc}}{2} - Q_{Cond}\right) \sqrt[3]{\frac{Kc_p}{2A^2 Q_{Nuc} g \rho_l^2 \beta} \left[L + \frac{L1 + L2}{2}\right]^{-1}} \quad (5)$$

For CAREM-25 conditions ($Q_{Nuc} \gg Q_{Cond}$) Eq. (5) shows that when decreasing the power level while keeping all other parameters constant, the core mean enthalpy approaches to saturation value, i.e. the core at low power levels is hotter than at nominal conditions (see Marcel et al. (2013)). This anti-intuitive result is related to the fact the core inlet enthalpy is not a controlled variable as in conventional reactors.

2.3.3. The flashing phenomenon

In CAREM-25, besides some vapor created in the core (the core exit vapor quality is practically zero) a certain amount of vapor is produced by the flashing phenomenon occurring in the chimney. As shown in Fig. 2, density differences between the cold and hot legs cause the water to flow without using pumps. Natural circulation is thus enhanced in this type of reactor by using a tall chimney. As the heated coolant flows upwards, the hydrostatic pressure decreases thus, the saturation temperature also decreases. When the saturation enthalpy becomes equal to the (constant) fluid enthalpy in the chimney, vapor created by flashing occurs, i.e. boiling out of the heated section, see Fig. 2. This ex-core boiling is enhanced as the reactor pressure decreases since at low pressure the saturation enthalpy is more dependent on the axial position. In CAREM-25 flashing is crucial for stability studies in both, the reactor start-up, i.e. at low pressure, and at nominal conditions. Let us add the flashing mechanism to the closed loop model described previously. Being P_{sys} the pressure at the highest part of the loop, i.e. at the entrance of the cooled section and neglecting the friction contribution, the hydrostatic pressure in the chimney section as a function of the axial location is given by

$$P(z) = P_{sys} + \rho g z \quad (6)$$

where z is the distance from the top of the heated section. Note that ρ is assumed constant in the chimney. This axial pressure change causes a variation of the saturation enthalpy along z, thus

$$h_{l,sat}(z) = h_{l,sat}(P(z)) = h_{l,sat}(P_{sys}) + \left.\frac{\partial h_{l,sat}}{\partial P}\right|_{P=P_{sys}} \rho g z \quad (7)$$

The onset of flashing will take place at $z = \lambda$ in the hot leg satisfying the following equality

$$h_{l,sat}(\lambda) = h_{Nuc,e} \quad (8)$$

with λ being the flashing boundary measured from the chimney top. The heat balances in the heated and cooled sections are then

$$Q_{Nuc} = \dot{m}(h_{Nuc,e} - h_{Nuc,i}) \quad (9)$$

$$Q_{SG} = \dot{m}(h_{l,sat}(P_{sys}) - h_{SG,e}) = \dot{m}(h_{l,sat}(P_{sys}) - h_{Nuc,i}) \quad (10)$$

By replacing Eqs. (9) and (10) into (3) we obtain an expression for the condensation power Q_{Cond} in the case the flashing effect is considered.

$$Q_{Cond} = \dot{m}(h_{Nuc,e} - h_{l,sat}(P_{sys})) \quad (11)$$

We can now use Eqs. (7), (8) and (11) to evaluate the point at which flashing starts. Thus

$$\lambda = \frac{Q_{Cond}}{\dot{m}} \frac{1}{\rho g \left(\partial h_{l,sat}/\partial P\right)\big|_{P=P_{sys}}} \quad (12)$$

By using Eq. (1) for describing the mass flow rate, Eq. (12) is transformed into (see Marcel et al. (2013))

$$\lambda = \frac{Q_{cond}}{\left(\partial h_{l,sat}/\partial P\right)\big|_{P=P_{sys}}} \sqrt[3]{\frac{Kc_p}{2A^2 Q_{Nuc} g^4 \rho_0^5 \beta [L + (L1 + L2)/2]}} \quad (13)$$

Eq. (13) has important implications: it is well known the importance of the location of the two-phase boundary in the void transport delay which is the basis of the density wave instability mechanism. The significance of the location of such a boundary is thus obvious.

By using CAREM-25 data and assuming the coolant is saturated at the core exit, the amount of power converted into vapor by means of flashing Q_{Cond} can be estimated as,

$$Q_{Cond} = \dot{m}(h_{l,sat,Ch,i} - h_{l,sat,Ch,e}) = 0.5\,\text{MW} \quad (14)$$

The presence of vapor flashing enhances self-pressurization of the system. If the vapor production rate is larger than the condensation rate the system pressure will increase and the flashing effect will diminish thus contributing to maintain the pressure constant. Vapor production in the chimney directly affects the gravitational pressure drop over this section, hence it is expected that Type-I feedback mechanism is amplified by the occurrence of void flashing.

3. The natural variables of the system

Since the behaviour of CAREM-25 is different from other water reactors (See Marcel et al. (2013) and IAEA (in press)), the use of the N_{sub} vs. N_{PCH} dimensionless plane for representing its stability performance might not be the optimal one. In this section, the best way of representing such a performance and its relation with the conventional dimensionless plane is discussed.

As shown in previous sections (see Marcel et al. (2013) for further details) the thermal-hydraulic behaviour of CAREM-25 reactor can be described by using three independent parameters, so-called natural variables. These are:

- The system pressure, P_{sys} (defined at the steam dome) which basically influences the fluid properties and the saturation enthalpy variation with the pressure,
- The nuclear core power, Q_{Nuc}, and
- The power which is condensed in the steam dome, Q_{Cond}.

Although this election is not unique, it has been proved to be very useful in practice since it immediately refers to controllable parameters of the system. In addition, for CAREM-25 reactor (at constant pressure), the use of the Q_{Cond} vs. Q_{Nuc} plane for constructing the stability maps enlarges the region of interest which is, on the contrary, a very narrow region in the conventional subcooling vs. phase change dimensionless plane, i.e. N_{Sub}vs. N_{PCH}, as it is shown later. From the definition of these two dimensionless numbers a direct relation with the natural variables of the system can be obtained. For simplicity, in the analysis shown in this section, the flashing effect is not considered. In this way,

$$N_{PCH} \equiv \frac{Q_{Nuc}}{\dot{m} h_{fg}} \frac{\rho_l - \rho_v}{\rho_v} \quad (15)$$

where h_{fg} is the latent heat of vaporization. Although it is not strictly the case, the natural circulation relation shown in Eq. (1),

which assumes a uniform heat flux in both the reactor core and in the steam generators neglecting the two phase contribution in the buoyancy force, can be used with reasonable accuracy (see Marcel et al. (2013)).

By using Eq. (1) for expressing the mass flow rate we obtain

$$N_{PCH} = \frac{1}{h_{fg}} \frac{\rho_l - \rho_v}{\rho_v} \sqrt[3]{\frac{Q_{Nuc}^2 Kc_p}{2A^2 g \rho_l^2 \beta} \left[L + \frac{L1 + L2}{2}\right]^{-1}} \tag{16}$$

Eq. (16) states the following relation exists between the phase change number and the core power

$$N_{PCH} \propto Q_{Nuc}^{2/3} \tag{17a}$$

And then,

$$Q_{Nuc} \propto N_{PCH}^{3/2} \tag{17b}$$

The same can be done for the subcooling number, which is defined as

$$N_{Sub} \equiv \frac{h_{l,sat} - h_{Nuc,i}}{h_{fg}} \frac{\rho_l - \rho_v}{\rho_v} \tag{18}$$

Eq. (5) can be easily transformed into

$$N_{Sub} = \left(\frac{h_{l,sat} - h_{Nuc,e}}{h_{fg}} + \frac{h_{Nuc,e} - h_{Nuc,i}}{h_{fg}} \right) \frac{\rho_l - \rho_v}{\rho_v} \tag{19}$$

By using Eq. (2), Eq. (19) can be rewritten as

$$N_{Sub} = \left(\frac{h_{l,sat} - h_{Nuc,e}}{h_{fg}} + \frac{Q_{Nuc}}{\dot{m} h_{fg}} \right) \frac{\rho_l - \rho_v}{\rho_v} \tag{20}$$

From which the phase change number can be easily identified. Thus,

$$N_{Sub} = \left(\frac{h_{l,sat} - h_{Nuc,e}}{h_{fg}} \right) \frac{\rho_l - \rho_v}{\rho_v} + N_{PCH} \tag{21}$$

The saturation enthalpy and the core exit enthalpy are related with the condensation power as (see Marcel et al. (2013))

$$h_{l,sat} - h_{Nuc,e} = -\frac{Q_{Cond}}{\dot{m}} \tag{22}$$

By replacing Eq. (22) into Eq. (21) and manipulating the expression we can write

$$Q_{Cond} = (N_{PCH} - N_{Sub}) \frac{\rho_v \dot{m} h_{fg}}{\rho_l - \rho_v} \tag{23}$$

By identifying the last term of Eq. (23) with Eq. (15) we see that

$$Q_{Cond} = (N_{PCH} - N_{Sub}) \frac{Q_{Nuc}}{N_{PCH}} \tag{24}$$

By manipulating Eq. (16) we get,

$$Q_{Nuc} = N_{PCH}^{3/2} \sqrt{\left(h_{fg} \frac{\rho_v}{\rho_l - \rho_v} \right)^3 \frac{2A^2 g \rho_l^2 \beta}{Kc_p} \left[L + \frac{L1 + L2}{2}\right]} \tag{25}$$

Finally by replacing Eq. (25) into Eq. (24) we can obtain the desired relation

$$Q_{Cond} = N_{PCH}^{1/2} (N_{PCH} - N_{Sub}) \sqrt{\left(h_{fg} \frac{\rho_v}{\rho_l - \rho_v} \right)^3 \frac{2A^2 g \rho_l^2 \beta}{Kc_p} \left[L + \frac{L1 + L2}{2}\right]} \tag{26}$$

And thus,

$$Q_{Cond} \propto N_{PCH}^{1/2} (N_{PCH} - N_{Sub}) \tag{27}$$

From this result it is clear that the condensation power has a certain relation with the core exit quality.

In order to stress the mapping obtained with the transformation of the N_{PCH} vs. N_{Sub} plane into the Q_{Nuc} vs. Q_{Cond} plane, the following approximate calculation is performed.

Recalling the energy balance in the system it is found that:

$$Q_{Nuc} = Q_{SG} + Q_{Cond} \tag{28a}$$

$$Q_{Nuc} = \dot{m}(h_{Nuc,e} - h_{Nuc,i}) \tag{28b}$$

$$Q_{SG} = \dot{m}(h_{sat} - h_{SG,e}) = \dot{m}(h_{sat} - h_{Nuc,i}) \tag{28c}$$

Eqs. (28) and (2) can be combined to show that

$$h_{sat} - h_{Nuc,i} = \frac{Q_{Nuc} - Q_{Cond}}{\dot{m}} = \frac{Q_{Nuc} - Q_{Cond}}{Q_{Nuc}^{1/3}} \sqrt[3]{\frac{Kc_p}{2A^2 g \rho_l^2 \beta} \left[L + \frac{L1 + L2}{2}\right]^{-1}} \tag{29}$$

By replacing Eq. (29) in Eq. (18) yields to

$$N_{Sub} = \frac{Q_{Nuc} - Q_{Cond}}{Q_{Nuc}^{1/3}} \frac{\rho_l - \rho_v}{h_{fg} \rho_v} \sqrt[3]{\frac{Kc_p}{2A^2 g \rho_l^2 \beta} \left[L + \frac{L1 + L2}{2}\right]^{-1}} \tag{30}$$

For most cases it can be stated that $Q_{Nuc} \gg Q_{Cond}$. By neglecting the condensation power in Eq. (30) we can write

$$N_{Sub} \approx Q_{Nuc}^{2/3} \frac{\rho_l - \rho_v}{h_{fg} \rho_v} \sqrt[3]{\frac{Kc_p}{2A^2 g \rho_l^2 \beta} \left[L + \frac{L1 + L2}{2}\right]^{-1}} \tag{31}$$

And finally the core power can be related to the subcooling number as

$$Q_{Nuc} \propto N_{sub}^{3/2} \tag{32}$$

The similarity between Eqs. (32) and (28b) is obvious and is explained by the fact CAREM-25 operational range is very close to the quality line equal to zero.

In addition to previous findings, another physical interpretation of the N_{Sub} can be explicitly written by identifying Q_{SG} in Eq. (30).

$$N_{sub} = \frac{Q_{SG}}{Q_{Nuc}^{1/3}} \frac{\rho_l - \rho_v}{h_{fg} \rho_v} \sqrt[3]{\frac{Kc_p}{2A^2 g \rho_l^2 \beta} \left[L + \frac{L1 + L2}{2}\right]^{-1}} \tag{33}$$

Since in the mass flow rate derivation from Eq. (1), single phase natural circulation is assumed (i.e. $Q_{Cond} \ll Q_{Nuc}$, Q_{SG}), in Eq. (21) Q_{Nuc} can be replaced by the power removed by the steam generators Q_{SG} (see Eq. (28a)) showing that

$$N_{sub} \propto Q_{SG}^{2/3} \tag{34}$$

To visualize the mapping defined by Eqs. (25) and (26), the following thermal-hydraulic stability maps are constructed (see Fig. 3). Such maps correspond to the stability performance of a natural circulation BWR reactor operated at constant pressure, with and without neutronic feedback (Van Bragt and Van der Hagen, 1998). In order to emphasize the region of interest (ROI), the CAREM-25 operational region is also showed.

As can be observed from the figure, the low quality region close to the single-phase boundary (i.e. the region of interest for the CAREM-25 reactor) is enlarged by using the proposed election of variables. In addition, the use of the Q_{Nuc} vs. Q_{Cond} plane also has the advantage of referring to the natural variables of the system which have a direct physical meaning. These results confirm the practical use of the Q_{Nuc} vs. Q_{Cond} plane instead of the common N_{PCH} vs. N_{Sub} plane for the case of self-pressurized, low quality, natural circulation reactors such as CAREM-25.

It needs to be pointed out that when considering a steady state condition, all thermal-hydraulic parameters of the system can be

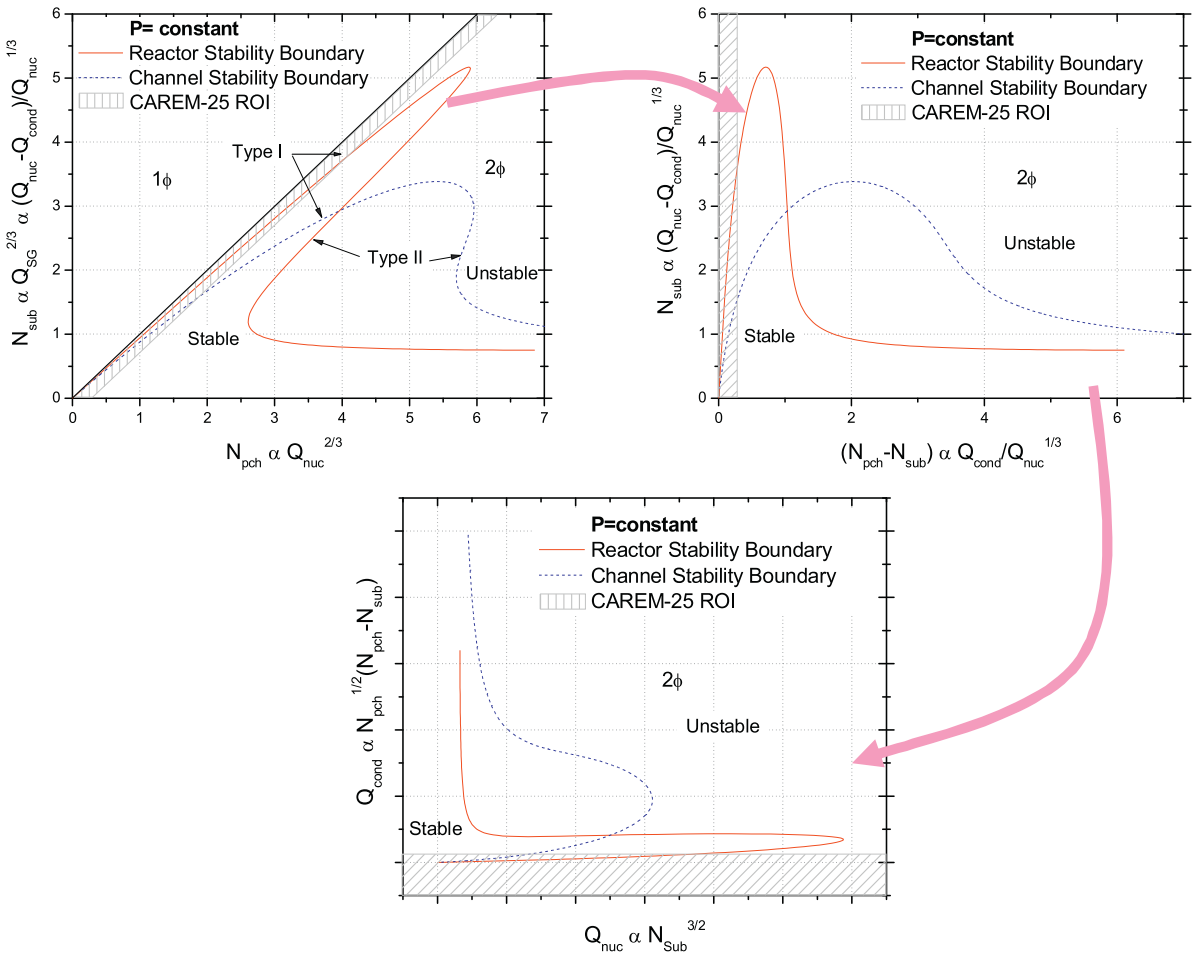

Fig. 3. The transformation of the N_{PCH} vs. N_{Sub} plane into the Q_{Nuc} vs. Q_{Cond} plane. It can be noted that the region of interested is enlarged with the proposed election of natural variables.

expressed in terms of the aforementioned natural variables (Marcel et al., 2013).

4. Numerical code

In this section the code used for the study of the reactor stability is briefly described. The so-called HUARPE code was developed by Zanocco et al. (2004a,b) to study the dynamics and stability of a reactor similar to CAREM-25, focusing on the behaviour of self-pressurization and the influence of diverse physical phenomena on the reactor stability. HUARPE includes modelling options in the time domain and in the frequency domain. With this code it is possible to create stability maps and to carry out parametric studies in different variables, being possible to assess the effect that those variables has on the system stability. In addition, it is possible to simulate transitory states and assess the system response to perturbations, and in such a way making possible to study, for example, oscillation maximum amplitudes and limit cycles.

The thermohydraulic finite-difference equations, programmed in the HUARPE code, are based on upwind differentiating over control volumes or nodes. In order to reduce the numerical diffusion implicit methods are avoided, as they demonstrated to be highly diffusive (Mahaffy, 1993). The explicit, first-order method is used instead: a cancellation effect, due to spatial and temporal numerical diffusion, is then achieved. The diffusion effect therefore decreases with increasing time-step size until a step function is perfectly propagated at the material Courant stability limit. In order to achieve this non-diffusive propagation, the code accounts with an "adaptive nodalization" scheme which consists of an iterative routine which nodalizes the system on the basis of the perturbations transport speed, satisfying the Courant limit in each volume. In this way it is possible to model the propagation of perturbations minimizing numerical diffusion effects.

It is interesting to study the influence of certain parameters on the system stability. In particular, it is a goal to investigate the influence in stability of the condensation power for a wide range of conditions.

In this document, the stability during start-up of a reactor with the aforementioned characteristics is studied, identifying the conditions that make it unstable.

4.1. Modelled hypothesis

The hypotheses considered in HUARPE code are listed below:

- One-dimensional flux is assumed, by modelling a special coordinate in the direction of flow circulation. This is applied in all circuit nodes, excepting the node that represents the mixture zone in the dome, since there is not a preferential direction of the flow circulation here. In this case, perfect mixing of the two-phase mixture is considered. The 1D assumption is considered to be conservative since in a 3D flow geometry the enthalpy fronts tend to dissipate more efficiently any perturbation which may lead to instabilities.

- The Drift-flux model is used for representing the two-phase flow dynamics. In the loop it is assumed that both phases behave as a mixture, with appropriately averaged properties and therefore, assuming the phases are in thermodynamic equilibrium. By neglecting subcooled boiling is considered to be conservative because of two different phenomena which effect will be discussed later: the neutronic feedback and the underestimation of the condensation power.
- For the saturated flow properties calculation the pressure change due to friction is neglected and such properties are only dependent on time and on hydrostatic position. In general, this is valid for circuits with natural circulation at low qualities. In the case of CAREM-25, the pressure change due to frictions is an order of magnitude lower than the change caused by height, and in the case of the chimney it can be of two orders of magnitude lower.
- "Carry under" is not considered from the dome to the inner part of the SGs. Due to the large size of the cross sectional area at the SGs inlet, it is expected that the flow speed will be low enough to avoid the carry under effect.
- Stratified flow is considered at the dome: the steam naturally will be accumulated at the upper part of the dome. The dome is thus divided into two variable volumes that represent the steam and the two-phase mixture zones. Each zone is represented by one node. At this place there is not a circulation preferential direction, due to the boiling and condensation processes that are expected to occur. It is also expected that these processes, together with the re-circulation caused by the volume control system, will favour mixing in the two-phase region. That is why averaged properties are considered in this mixture zone, assuming a perfectly mixed volume. Because of the self-pressurization, the correct modelling of the interaction between phases is important for low-condensation regimes; therefore, a non-equilibrium model is included to account for the interaction between the two volumes. The dome has its own dynamic behaviour and interacts with the rest of the cooling circuit through mass exchanges with the chimney and the steam generator inlet.
- The fuel structure is assumed to be one dimensional, and it is nodalized in the axial direction. It is considered that the fuel is homogeneous (mixed cladding and pellet) and the thermal conductivity is independent from temperature. The time derivative of the fuel temperature is therefore proportional to the difference between the power generated and that exchanged. An axial temperature profile is modelled, neglecting axial conduction within the fuel (see Zanocco et al. (2004a) for further details).
- It is supposed that the core power has a cosinoidal-type distribution with the maximum moved to the lower part. This is expected due to different phenomena which affect the power distribution such as: the control rods position, the void fraction at the vicinity of the core outlet, and the effects related with neutron leakage at the core ends.
- A point-kinetics model with 6 delayed neutron groups for the core power is used. Reactivity feedbacks caused by coolant density and fuel temperature are contemplated.
- It is expected that in the lower plenum there are mixing processes which enhance enthalpy fronts diffusion coming from the SGs. This process is ruled by a strongly three-dimensional geometry, which makes it difficult to model. When the enthalpy fronts diffusion is not considered, however, a conservative approximation from the stability point of view is obtained. Therefore, the mixing process in the lower plenum is not included in the circuit.
- It is considered that the power extracted by the SGs is constant and axially uniform.

Further details regarding the model can be found in Zanocco et al. (2004a).

5. Linear stability results

The analysis referred to CAREM-25 reactor stability is presented building the so-called stability maps. The preparation of such stability maps is carried out by using the power generated in the core (Q_{Nuc}) as abscissa variable, and the power extracted by condensation in the region of the steam dome (Q_{Cond}) as ordinates variable. As mentioned in previous section, such an election is preferred instead of the dimensionless sub-cooling number N_{Sub} and phase change number N_{PCH} since CAREM-25 operational region is a very narrow region close to the steam quality line equal to zero, which makes its perception difficult (see Fig. 3). Besides, the natural variables of the system are Q_{Nuc} and Q_{Cond}, which make the stability maps comprehension easy and enable an optimal visualization of the area of interest: wide range in Q_{Nuc} with low values of Q_{Cond}.

By perturbing a linear system, it may progress in several ways: it may oscillate (or not) and it may present growing or decaying amplitude behaviour. The evolving of a dynamic response can be adjusted using an exponential function of e^{at^*} kind, with t^* being the dimensionless time. From this, it can be defined the amplification factor a, which is used in this document to define the system stability: positive values are equivalent to unstable conditions, and negative values to stable cases. In addition $a = 0$ defines the stability boundary. In this document the stability maps are presented as contour plots with the amplification factor a as the vertical axis. Moreover, the colour in the plots represents the level of the vertical coordinate. The dynamic response of the system can also be used to extract the natural frequency of the response which can help determining the nature of the instability mechanism.

5.1. Stability at nominal conditions (P = 12.25 MPa) – a parametric study

In this section, the CAREM-25 linear stability performance at nominal pressure is investigated. In order to clarify the effects derived from the different feedback mechanisms, three cases are considered. These are:

- The purely thermal-hydraulic stability.
- The neutronic-thermal-hydraulic stability (thermal-hydraulic stability with the neutronic feedback).
- The reactor stability (thermal-hydraulic stability with the neutronic and pressure feedback).

5.1.1. The purely thermal-hydraulic stability

In previous researches, it has been shown that beyond a certain condensation power level, for which the two-phase boundary λ is located in the last part of the chimney, the system shows a significant increment in the amplification factor (see e.g. Zanocco et al., 2004a). This happens when, without boiling in the core, enthalpy outside the core is higher than the saturation enthalpy at the chimney outlet, producing vapor by means of flashing. The presence of void fraction in the chimney generates an increment in the buoyancy force. The higher the void fraction is, the lower the average density in the hot leg is and thus the higher is the buoyancy force. If the two-phase boundary λ is located in the chimney, the sensibility of the buoyancy force to changes in the coolant enthalpy therefore increases. This is due to the fact a slight perturbation in the core outlet enthalpy causes a great movement of λ, which in turn produces a great variation of the buoyancy force. This effect tends to destabilize the system, incrementing the amplification factor which shows a maximum value when λ is located in the central region of the chimney and a minimum value when λ is close to the chimney outlet and deep inside the core section. For this reason, when the system is unstable, i.e. λ is placed in the central region of the chimney, it can be stabilized both by increasing or decreasing

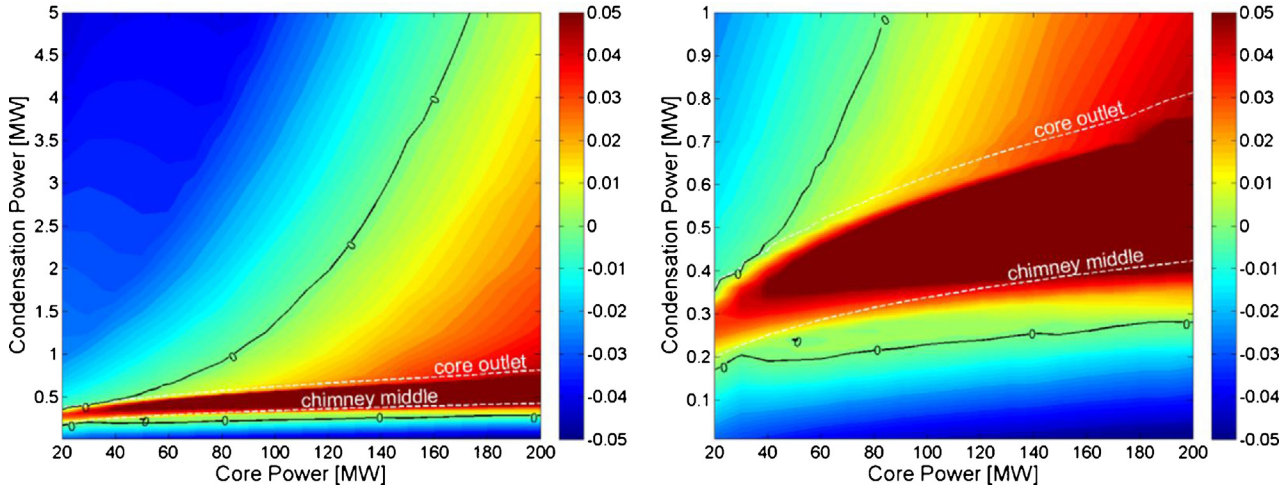

Fig. 4. The thermal hydraulic stability map, expressed in terms of the amplification factor for the case in which neither neutron nor pressure feedback have been considered. The white lines show the cases in which the two-phase line is located at the core outlet and the chimney middle.

Q_{Cond}. This effect is shown in Fig. 4, which shows the case in which neither the neutron nor the pressure feedback pressure have been considered in the system. As can be observed for any core power there are two condensation powers for which the stability line is crossed.

In order to point out the two-phase region in the system, in the following plots presented in this document, the points for which the two-phase boundary coincides with the core outlet location and also the chimney middle location are included.

As can be noted, the lower the condensation power Q_{Cond} is, the closer is λ regarding the chimney outlet. This result agrees with the analytical relation (valid for cases in which only exists vapor generated by flashing, i.e. λ is located in the chimney) given by Eq. (13).

From this analysis it is clear that the system is unstable when λ is located in a wide range of values, starting from positions which are close to the last quarter of the chimney and extending to cases in which boiling takes place in the core. By lowering Q_{Cond} the two-phase region becomes smaller, reducing the void fraction contribution in the buoyancy force; and therefore, reducing its relative sensibility. For this reason, the oscillations are more efficiently damped, emerging a stability area.

Analysing the system dominant frequency in the considered map it is possible to elucidate the nature of the instability mechanism. In Fig. 5 the level in the contour plot corresponds to the ratio

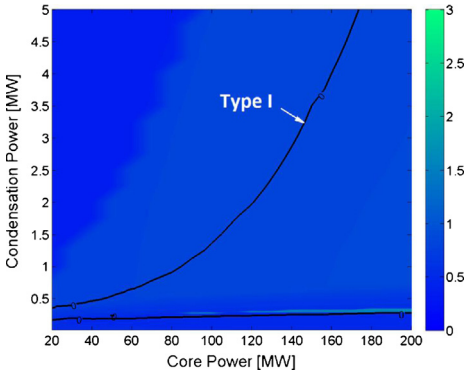

Fig. 5. Ratio of the period of the instability cycle and the residence time of a fluid particle in the chimney section corresponding to the cases shown in the stability map from Fig. 3, i.e. when neither neutron nor pressure feedbacks have been considered. The white lines show the cases in which the two-phase line was located at the core outlet and the chimney middle location.

of the residence time of a fluid particle in the chimney section and the period of the instability cycle. As can be noted such a parameter is within 0.5–1 for the whole unstable region in the map, indicating the mechanism responsible for the aforementioned instabilities corresponds well with density waves travelling through the reactor chimney (Marcel et al., 2008; Marcel, 2007). This result also confirms the dominant instability mechanism is due to Type I DWO. This result also agrees with previous findings for natural circulation BWR channel stability analysis (see Fig. 3).

5.1.2. The neutronic-thermal-hydraulic stability

In order to study the core dynamic influence in the system stability, the thermal model of the fuels and the corresponding neutronic feedback is included. The resulting stability map is shown in Fig. 6.

One of the most important effects in this case is the neutronic feedback due to coolant density changes: in the case of having a constant heat flux condition, an increment in the core flow is followed by an enthalpy decrease at the chimney outlet and, consequently, an increment in the coolant average density. When the neutronic feedback is included, a reactivity insertion is produced due to the fact the reactivity coefficient due to coolant density, r_ρ is positive. Thus, the power by fission increases and therefore increases the enthalpy at the core outlet, which tends to balance the thermal hydraulic effect, stabilizing the system. Besides, the neutronic feedback also presents a faster response compared to the dynamics of the density waves travelling through the chimney. This is due to the fact an average coolant density change affects the nuclear core power before the arrival of the enthalpy front to the chimney inlet. This reduces the associated phase delay. The explained phenomenon provides a stabilizing effect for low frequency Type-I oscillations, which dominate when Q_{Cond} is small.

When Q_{Cond} increases, the amount of void in the core increases and the neutronic feedback becomes more important. When the neutronic feedback is too strong, however, oscillations of higher frequencies take place, and the system is relatively destabilized by the Type-II instability mechanism.

The core dynamics provides a stabilizing effect in the system regarding the unstable region induced by flashing phenomenon since the size of the unstable region decreased.

In Fig. 7 the ratio of the residence time of a fluid particle in the chimney section and the period of the instability cycle is plotted for the case the neutronic feedback is included in the model.

As can be noted from Fig. 7, the mechanism responsible for the low condensation power unstable region corresponds well with

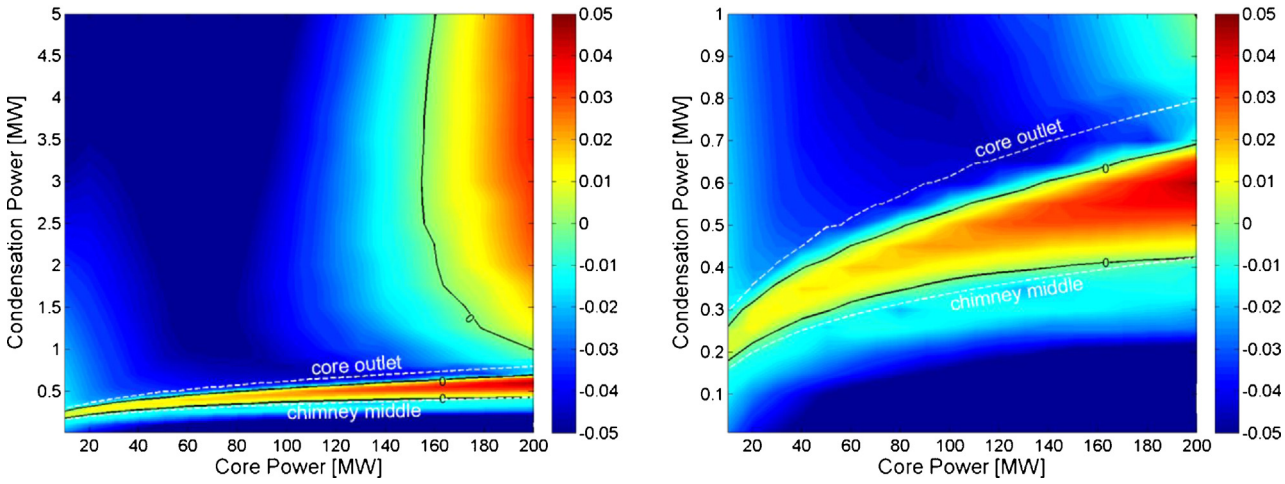

Fig. 6. Neutronic-thermal-hydraulic stability map, expressed in terms of amplification factor for the case in which it is considered the neutronic feedback but not the pressure feedback. The white lines show the cases in which the two-phase line is located at the core outlet and the chimney middle.

density waves travelling through the reactor chimney. In contrast, the high condensation power unstable region is characterized by higher ratios of the residence time of a fluid particle in the chimney section and the period of the instability cycle, which corresponds well with the Type-II instability mechanism. This result is a direct consequence of the high frequency neutronic feedback. When λ moves downwards into the core, the neutron feedback becomes dominant, causing higher natural frequencies in the system. The associated period is now related with the characteristic time associated with the residence time of a fluid particle in the core section.

The aforementioned results agree well with previous findings for natural circulation BWR stability analysis (see Fig. 3).

5.1.3. The reactor stability

The effect of pressure feedback is expected to cause a stabilizing effect regarding the case of considering constant pressure (which is equivalent to assume an infinite steam volume). Such an effect responds to the following mechanism: an increment of the void fraction in the chimney expands the entire coolant, pressurizing the system. The system pressure increments the saturation enthalpy which tends to reduce the void fraction. Therefore, the pressure feedback natural effect is to balance the density changes of the two-phase region. The feedback in pressure is stronger when the steam volume is lower and when the vapour production is larger.

Fig. 8 shows the CAREM-25 reactor stability map for the case in which both the neutronics and the pressure feedback effect are included in the simulation. In this manner, all relevant mechanisms determining the reactor dynamic behaviour are taken into account.

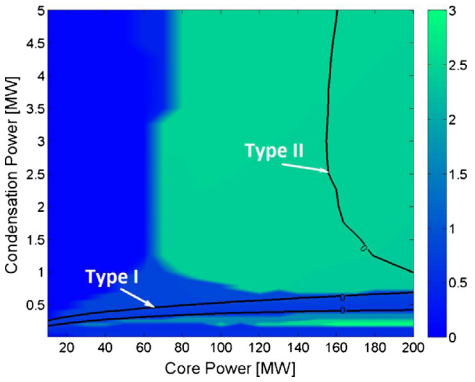

Fig. 7. Ratio of the period of the instability cycle and the residence time of a fluid particle in the chimney section corresponding to the cases shown in the stability map from Fig. 5, i.e. when the neutronic feedback is considered but not the pressure feedback.

As it can be seen, the feedback pressure effect stabilizes the system. By comparing Figs. 6 and 8, it can be noted the unstable region is clearly reduced. In addition, the low Q_{Cond} unstable region is still bounded by the region defined by the core outlet and the chimney middle point.

Fig. 9 presents the results of the ratio of the residence time of a fluid particle in the chimney section and the period of the instability cycle corresponding to the case the neutronic feedback and the pressure feedback are included in the model. As can be noted, in the unstable region, the ratio is again within 0.5 and 1. This suggests the most important mechanism in the stability of the system is again due to density waves corresponding to the Type-I mechanism.

The previously obtained results are promissory regarding CAREM-25 reactor stability performance since they show a large region at which the system can be operated with sufficient stability margins. In needs to be remarked that such a margin may be considerably incremented by slightly incrementing the condensation power at the dome. In this way, the reactor operational point may be tuned, thus optimizing its stability performance.

Because of this result, it has been decided to implement a condensation device in the reactor steam dome in order to ensure a minimum condensation power at any condition regarding nominal pressure.

5.2. Stability analysis at low pressure (4.7–12.25 MPa)

During the pressurization stage the unbalanced power (regarding the generated power in the core and the power removed by the steam generators) need to increase. Such an increment produces an increase in the vapor production which in turn causes a given pressurization rate. As shown by Marcel et al. (2013) at steady state conditions an increase in the condensation power produces a similar effect. In this section, steady state stability maps are used to evaluate the stability performance at pressurization conditions. It has to be kept in mind, however, that such an analysis assumes slow pressurization ramps, in which the system can be considered to be in quasi-stationary conditions. Obviously, an effective condensation power which has to be greater than the real one should be considered during the pressurization stage. In other words, since the pressurization is achieved by incrementing the power released by the core, the location of the two-phase boundary tends to move downwards. From this analysis it is clear that by using the linear stability maps the results are conservative.

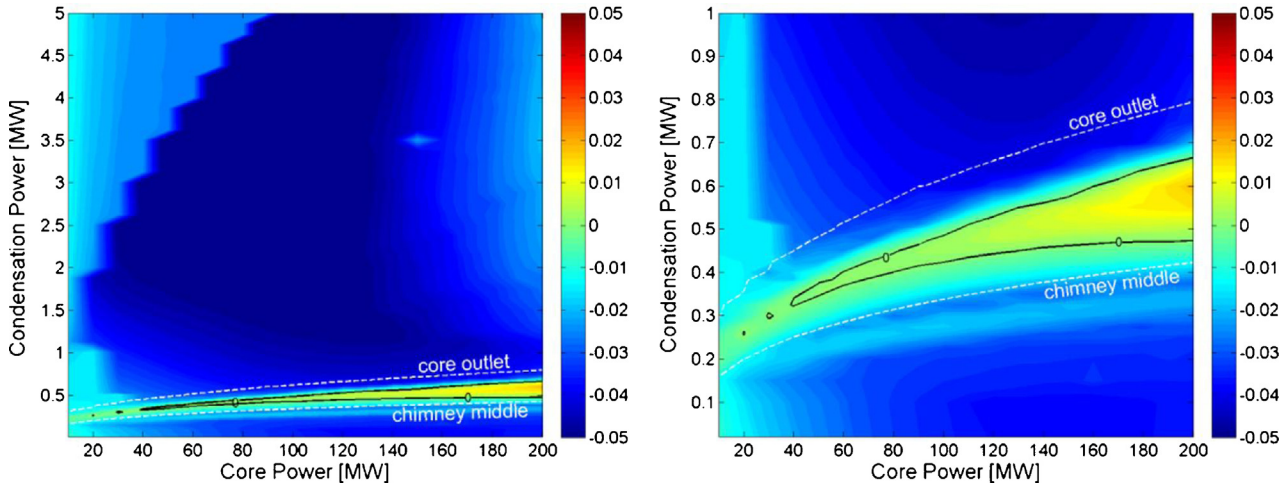

Fig. 8. Reactor stability map, for the case in which both the core dynamic and the feedback in pressure are considered. The white lines show the cases in which the two-phase line is located at the core outlet and the chimney middle.

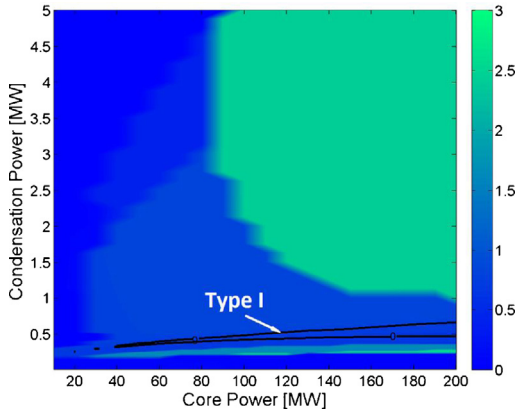

Fig. 9. Ratio of the residence time of a fluid particle in the chimney section and the period of the instability cycle corresponding to the cases shown in the stability map from Fig. 7. The neutronic and pressure feedback are considered.

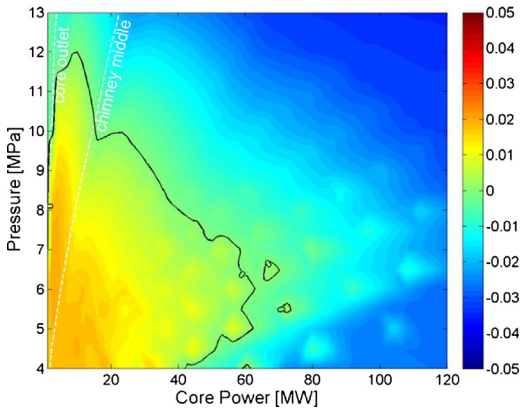

Fig. 10. Stability map at Q_{Cond} = 0.2 MW. The white lines show the cases in which the two-phase line is located at the core outlet and the chimney middle.

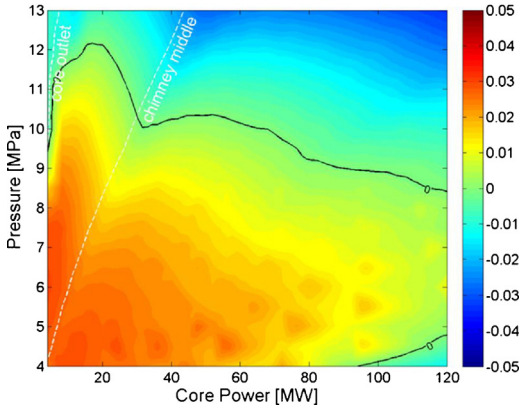

Fig. 11. Stability map at Q_{Cond} = 0.25 MW. The white lines show the cases in which the two-phase line is located at the core outlet and the chimney middle.

Here, instead of representing the stability results in the Q_{Nuc} vs. Q_{Cond} plane, a second type of plot is constructed. In this second modality Q_{Nuc} and P are taken as variables, keeping Q_{Cond} constant, which enables a better characterization of the system during a heating ramp. This is due to the fact that during the pressurization stage, it is expected that P will vary depending on power misbalances (IAEA, in press). For this reason it is useful to visualize a wide range of Q_{Nuc} and P at a value of Q_{Cond} defined as constant. This assumption is supported by the fact Q_{Cond} is a parameter which is planned to be regulated during start-up.

5.2.1. Stability maps in Q_{Nuc}–P

Figs. 10–15 show stability maps obtained at different Q_{Cond} values.

From the figures it is immediately observed the pressure stabilizing effect. In the investigated range of Q_{Cond}, it can be seen that at high P values the system is stable, regardless the value taken by the core power Q_{Nuc}.

Fig. 10 shows a stable region at middle to high Q_{Nuc} values, despite the pressure at which it is operated. This is related to the fact the flow quality in this region is very low (see Eq. (27)) and therefore the density wave instability mechanism cannot destabilize the system (the two-phase contribution to the buoyancy term of the momentum equation is very small). When slightly increasing the condensation power, however, a great change in shape is observed. Between Figs. 10 and 11 Q_{Cond} varied only 0.05 MW, but the area of the unstable region in the maps incremented more than the double in size.

Figs. 12–15 also show the unstable region moves when further increasing Q_{Cond}. This is explained by the movement of the two-phase region (accounted by the value of λ) which affects both the magnitude and the phase of the feedback mechanism responsible of the density wave instability. In this manner, λ locates at different

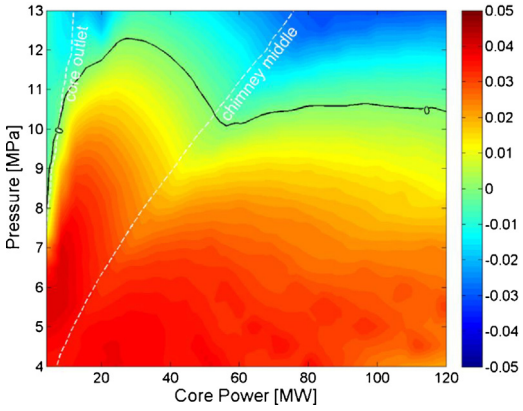

Fig. 12. Stability map at Q_{Cond} = 0.3 MW. The white lines show the cases in which the two-phase line is located at the core outlet and the chimney middle.

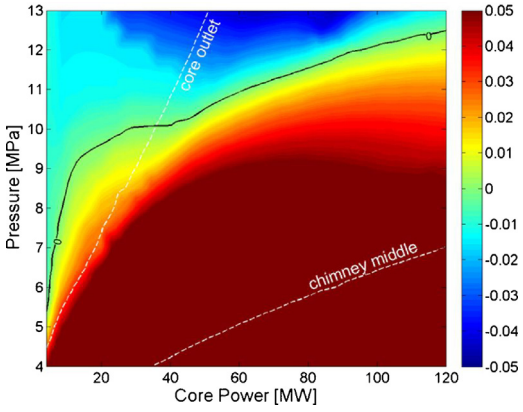

Fig. 13. Stability map at Q_{Cond} = 0.5 MW. The white lines show the cases in which the two-phase line is located at the core outlet and the chimney middle.

positions in the hot leg, inducing different feedback mechanisms. It is thus clear that Q_{Cond}can be an excellent parameter to 'tune' the system in order to demote the density wave instability mechanism, optimizing the system stability performance. In particular, it is observed that for Q_{Cond} higher than 0.75 MW it is possible to go from low P and low Q_{Nuc} to high P and high Q_{Nuc} without encountering instabilities (IAEA, in press).

Moreover, the maps presented in the Q_{Nuc} and P plane do not show significant changes when incrementing Q_{Cond} from 0.75 MW to 1.0 MW.

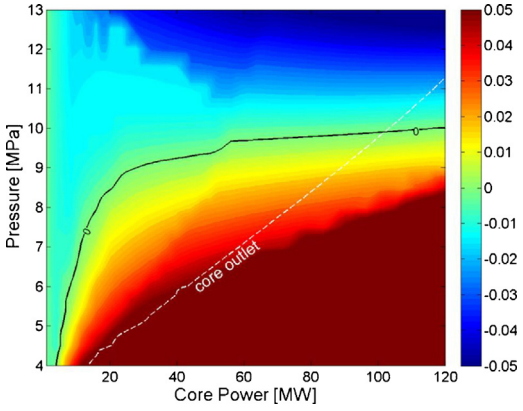

Fig. 14. Stability map at Q_{Cond} = 0.75 MW. The white line shows the cases in which the two-phase line is located at the core outlet.

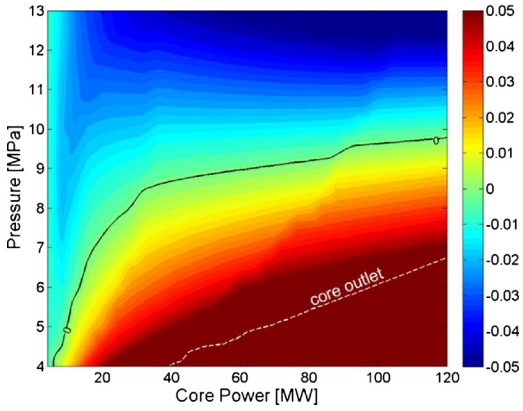

Fig. 15. Stability map at Q_{Cond} = 1.0 MW. The white line shows the cases in which the two-phase line is located at the core outlet.

6. Conclusions

In this work, different stability maps obtained from a linearized model are presented. It is shown that the flashing effect is crucial to correctly investigate the stability performance of a self-pressurized, low quality natural circulation reactor such as CAREM-25 reactor. In addition, it is verified that, in the region of interest, the dominant destabilizing mechanism is due to density waves travelling through the chimney section corresponding to Type-I instabilities. The stabilizing effects due to the neutronic feedback and the reactor pressure have been verified at nominal conditions.

It is found that the condensation taking place in the steam dome has a great impact in defining the stability of the reactor and thus can be used to tune the CAREM-25 operational point. For this reason, to enhance the reactor stability performance, a condensation device might be used to increase the power condensed in the pressure vessel dome. Preliminary estimations show that incrementing the condensed power up to 0.75 MW would be enough to increase the reactor stability margins and thus optimize the plant safety.

The stability maps presented in terms of Q_{Nuc} and P enabled a clear visualization of a possible trajectory for the start-up stage. From the results it is observed that pressure has a stabilizing effect since by incrementing P it is possible to reach a stable condition regardless the value of Q_{Nuc}. In addition, it can be concluded it is desirable to increase as much as possible the pressure of the operational point from which the reactor needs to begin the start-up phase. A remarkable result is the effect that Q_{Cond} has on the system when Q_{Nuc} is varied. It is observed that the system is very sensitive to the value of Q_{Cond}. In particular, when Q_{Cond} is equal to 0.2 MW, by increasing Q_{Nuc} the system tends to be stabilized and the opposite occurs for Q_{Cond} higher than 0.5 MW. This result is related to the positioning of the two-phase boundary in the hot leg, which may promote or demote the instabilities.

It is found that the maps presented in the Q_{Nuc} and P plane do not show significant changes when incrementing Q_{Cond} from 0.75 MW to 1.0 MW. In addition, these maps also show the reactor may be operated from a condition of low P and low Q_{Nuc} to a nominal condition of P and Q_{Nuc}, without passing through unstable region if a condensation power level of at least 0.75 MW can be guaranteed. This important result indicates the reactor can be started-up without observing instabilities of thermal hydraulic origin.

References

Delmastro, D., 2008. Thermal-hydraulic aspects of self-pressurized natural circulation integral reactors. In: Proc. of Int. Workshop on Thermal-Hydraulics of Innovative Reactor and Transmutation Systems – THIRS, Eggenstein-Leopoldshafen, Germany, 14–16 April.

Gomez, S., 2000. Development activities on advanced LWR designs in Argentina. In: Technical Committee Meeting on Performance of Operating and Advanced LWR Designs, Munich, Germany. IAEA Pub, pp. 113–120.

Guanghui, S., Dounan, J., Fukuda, K., Yujun, G., 2001. Theoretical Study on density wave oscillation of two phase natural circulation under low quality conditions. J. Nucl. Sci. Technol. 38 (8), 607–613.

Guanghui, S., Dounan, J., Fukuda, K., Yujun, G., 2002. Theoretical and experimental study on density wave oscillation of two-phase natural circulation of low equilibrium quality. Nucl. Eng. Des. 215, 187–198.

International Atomic Energy Agency (IAEA), 2013. Advanced Water Cooled Reactor Case Studies in Support of Passive Safety Systems. IAEA-TECDOC-1705, IAEA, Vienna (in press).

Iida, H., Ishizaka, Y., Kim, Y.C., Yamaguchi, C., 1994. Design study of the deep-sea reactor X. Nucl. Technol. 107, 38–48.

Junli, G., Suizheng, Q., Guanghui, S., Dounan, J., 2006. Theoretical investigation on the steady state natural circulation characteristics of a new type of pressurized water reactor. Nucl. Sci. Tech. 17 (5), 314–320.

Kusunoki, T., Olano, N., Yoritsune, T., Ishida, T., Hoshi, T., Sako, K., 2000. Design of advanced integral-type marine reactor MRX. Nucl. Eng. Des. 201 (2), 155–175.

Lee, D., 2000. Design and safety of a small integral reactor (SMART). In: Int. Workshop on Utilization of Nuc. Power in Oceans, Tokyo, Japan, February 21–24.

Mahaffy, J.H., 1993. Numerics of codes: stability, diffusion and convergence. Nucl. Eng. Des. 145, 131–145.

Marcel, C.P., 2007. Experimental and Numerical Stability Investigations on Natural Circulation Boiling Water Reactors. IOS Press, Amsterdam, The Netherlands.

Marcel, C.P., Rohde, M., Van der Hagen, T.H.J.J., 2008. Experimental investigation on the ESBWR stability performance. Nucl. Technol. 164 (November).

Marcel, C.P., Rohde, M., Van Der Hagen, T.H.J.J., 2009. Experimental and numerical investigations on flashing-induced instabilities in a single channel. Exp. Therm. Fluid Sci. 33, 1197–1208.

Marcel, C.P., Delmastro, D.F., Furci, H., Masson, V.P., 2013. Stability of self-pressurized, natural circulation, low thermo-dynamic quality, nuclear reactors: phenomenology involved in the thermal-hydraulics of the CAREM-25 reactor. Nucl. Eng. Des. 254, 218–227.

Van Bragt, D.D.B., Van der Hagen, T.H.J.J., 1998. Stability of natural circulation BWRs: Part I. Description stability model and theoretical analysis in terms of dimensional groups. Nucl. Technol. 121, 40.

Zanocco, P., Delmastro, D., Giménez, M., 2004a. Modeling aspects in linear stability analysis of a self-pressurized natural circulation integral reactor. Nucl. Eng. Des. 231, 283–301.

Zanocco, P., Delmastro, D., Giménez, M., 2004b. Linear and nonlinear stability analysis of a self-pressurized, natural circulation, integral reactor. In: ICONE12, Int. Conf. Nuc. Eng., Washington, DC.